PNNL-15831

Pacific Northwest
National Laboratory
Operated by Battelle for the
U.S. Department of Energy

Comparison of LaBr3:Ce and NaI(Tl) Scintillators for Radio-Isotope Identification Devices (Revision 0)

B. D. Milbrath
J. E. Fast
R. T. Kouzes
B. J. Choate,
W. K. Hensley
J. E. Schweppe

April 2006

Prepared for the U. S. Department of Homeland Security
U.S. Customs and Border Protection and Domestic Nuclear Detection Office under U.S. Department of Energy Contract DE-AC05-76RL01830

DISCLAIMER

PACIFIC NORTHWEST NATIONAL LABORATORY
operated by
BATTELLE
for the
UNITED STATES DEPARTMENT OF ENERGY
under Contract DE-AC05-76RL01830

Printed in the United States of America

Available to DOE and DOE contractors from the
Office of Scientific and Technical Information,
P.O. Box 62, Oak Ridge, TN 37831-0062;
ph: (865) 576-8401
fax: (865) 576-5728
email: reports@adonis.osti.gov

Available to the public from the National Technical Information Service,
U.S. Department of Commerce, 5285 Port Royal Rd., Springfield, VA 22161
ph: (800) 553-6847
fax: (703) 605-6900
email: orders@ntis.fedworld.gov
online ordering: http://www.ntis.gov/ordering.htm


This document was printed on recycled paper.
(8/00)

Pacific Northwest National Laboratory
Operated by Battelle for the U.S. Department of Energy

Radiation Portal Monitor Project

Comparison of $LaBr_3$:Ce and NaI(Tl) Scintillators for Radio-Isotope Identification Devices

(Revision 0)

B. D. Milbrath, B. J. Choate,
J. E. Fast, W. K. Hensley,
R. T. Kouzes, J. E. Schweppe

April 18, 2006

PIET-43741-TM-488
PNNL-15831

Prepared for the U. S. Department of Homeland Security
U.S. Customs and Border Protection and Domestic Nuclear Detection Office
under U.S. Department of Energy Contract DE-AC05-76RL01830

Pacific Northwest National Laboratory
Richland, Washington 99352

SUMMARY

Lanthanum halide ($LaBr_3$:Ce) scintillators offer significantly better resolution (<3 percent at 662 kilo-electron volt [keV]) relative to sodium iodide (NaI(Tl)) and have recently become commercially available in sizes large enough for the hand-held radio-isotope identification device (RIID) market. There are drawbacks to lanthanum halide detectors, however. These include internal radioactivity that contributes to spectral counts and a low-energy response that can cause detector resolution to be lower than that of NaI(Tl) below 100 keV. To study the potential of this new material for RIIDs, we performed a series of measurements comparing a 1.5×1.5-inch $LaBr_3$:Ce detector with an Exploranium GR-135 RIID, which contains a 1.5×2.2-inch NaI(Tl) detector. Measurements were taken for short time frames, as typifies RIID usage. Measurements included examples of naturally occurring radioactive material (NORM), typically found in cargo, and special nuclear materials. Some measurements were noncontact, involving short distances or cargo shielding scenarios. To facilitate direct comparison, spectra from the different detectors were analyzed with the same isotope identification software (ORTEC ScintiVision™).

In general, the $LaBr_3$:Ce detector was able to find more peaks and find them faster than the NaI(Tl) detector. To the same level of significance, the $LaBr_3$:Ce detector was usually two to three times faster. The notable exception was for 40K-containing NORM where interfering internal contamination in the $LaBr_3$:Ce detector exist. NaI(Tl) consistently outperformed $LaBr_3$:Ce for this important isotope. $LaBr_3$:Ce currently costs much more than NaI(Tl), though this cost-difference is expected to diminish (but not completely) with time. As is true of all detectors, $LaBr_3$:Ce will need to be gain-stabilized for RIID applications. This could possibly be done using the internal contaminants themselves. It is the experience of the authors that peak finding software in RIIDs needs to be improved, regardless of the detector material.

ACKNOWLEDGMENTS

The authors appreciate helpful conversations with M. Mayhugh of Saint-Gobain and R. Arlt of the International Atomic Energy Agency.

CONTENTS

FIGURES AND TABLES

Figures

Tables

ACRONYMS AND ABBREVIATIONS

ANSI	American National Standards Institute
HEU	highly enriched uranium
keV	kilo-electron volt
$LaBr_3$:Ce	lanthanum bromide
LaCl3:Ce	lanthanum chloride
NaI(Tl)	sodium iodide
NORM	naturally occurring radioactive materials
RIID	radio-isotope identification device
WGPu	weapons-grade plutonium

1.0 INTRODUCTION

With resolution of approximately 3 percent at 662 kilo-electron volt (keV), lanthanum bromide ($LaBr_3$:Ce) scintillators (van Loef et al. 2001a, Shah et al. 2003a) offer a substantial improvement over sodium iodide (NaI[Tl]) scintillators, whose resolution is approximately 6-7 percent in comparable sizes. Growing the crystals has proven somewhat difficult, but they are now available commercially in sizes up to 2×2 inches from Saint-Gobain (Saint-Gobain Crystals and Detectors, Nemours, France). Another lanthanum halide, $LaCl_3$:Ce, has a resolution that is not quite as good but still approximately 4 percent (van Loef et al. 2001b, van Eijk 2001, Shah et al. 2003b), and is commercially available in similar sizes. As such, the lanthanum halides are at a size large enough for use in hand-held radio-isotope identification devices (RIIDs), an application currently dominated by NaI(Tl). Other alternative detector materials for RIID applications include the higher-resolution solid-state detectors high-purity germanium detector and cadmium zinc telluride. High-purity germanium detector is heavy and expensive, due to the need for cryogenic cooling, while it has proven difficult to scale up cadmium zinc telluride to sizes needed for RIIDs and still retain its advantageous high resolution (Syntfeld et al. 2005).

Unfortunately, the lanthanum halide scintillators have a few drawbacks of their own: internal radioactivity and a low-energy response that results in the resolution being lower than that of NaI(Tl) below approximately 100 keV. The internal radioactivity is due to naturally occurring radioisotopes ^{138}La and ^{227}Ac (Milbrath et al. 2005a, 2005b; Hartwell and Gehrke 2005; Kernan 2004). ^{138}La, which makes up 0.09 percent of naturally occurring lanthanum, has a 1.06 x 10^{11}-year half-life and produces two gamma rays: a 788.7-keV gamma ray from beta decay (34 percent) to stable ^{138}Ce and a 1435.8-keV gamma ray from electron capture (66 percent) to stable ^{138}Ba. There are also strong Ba K x-rays from 31-38 keV. ^{227}Ac has a 21.77-year half-life and occurs naturally as part of the ^{235}U decay series (Firestone and Ekstrom 2004). Chemically, actinium is very similar to lanthanum and is directly below it on the periodic table, which is why this contaminant is found in the scintillator. ^{227}Ac's decay chain to stable ^{207}Pb includes five alpha decays. Initial commercially available lanthanum halide crystals had a contamination level of 1.3 x 10^{-13} ^{227}Ac atoms/La atom (Milbrath et al. 2005b). This has since been reduced by over two orders of magnitude (Millbrath et al. 2005a, Iltis et al. 2004), but as shown in this report, still affects background spectra.

Early investigations of the lanthanum halides revealed that, despite their superior resolution at higher energies, the resolution is lower than that of NaI(Tl) at low energies, with the crossover occurring at approximately 100 keV (Balcerzyk et al. 2005, Figure 5; Dorenbos et al. 2004). This is due to two factors. One is that the lanthanum halides, while having very good light-yield proportionality in general, relative to NaI(Tl) show a sharp drop in proportionality below 20 keV. A second factor contributing to the superior resolution of NaI(Tl) at low energies is the fact that NaI(Tl) has a significantly larger light yield than the lanthanum halides below approximately 200 keV due to nonproportionality in NaI(Tl)'s response.

RIIDs have many uses such as hazardous material control, emergency response, medical applications, waste management, and homeland security. The role of RIIDs in the latter application (McDonald et al. 2004, Kouzes 2004) has, for obvious reasons, generated much interest of late. In addition, the American National Standards Institute (ANSI) has developed new standards for RIIDs (ANSI 2003). These factors have resulted in much effort by the various commercial suppliers to improve their RIIDs and continuous efforts by others to evaluate their performance (Woodring et al. 2004, Seitz et al. 2005). Thus, we were motivated to investigate

what improvement, if any, $LaBr_3Ce$ could bring to RIIDs, especially for naturally occurring radioactive material (NORM) and threat identification, given both its improved resolution and aforementioned drawbacks. The final results of that investigation are reported in this document, building on earlier preliminary findings (Milbrath et al. 2005c).

2.0 DETECTOR COMPARISON STUDY

For our study, we obtained a 1.5×1.5-inch $LaBr_3$:Ce scintillator directly coupled to a 2-inch-diameter Hamamatsu R6231 photomultiplier tube from Saint-Gobain. We measured this detector to have a resolution of 2.7 percent at 662 keV. This detector cost nearly US $10,000, making it much more expensive than a comparably sized NaI(Tl). Saint-Gobain hopes to eventually be able to price this material comparably to bismuth germinate [a few times that of NaI(Tl) for this size].(a) For our NaI(Tl) measurements, we used a commercially available RIID, the Exploranium GR-135 (SAIC Exploranium, Mississauga, ON, Canada). The NaI(Tl) detector in this device is 1.5×2.2 inches and has a resolution of 6.5 percent at 662 keV. Though of different sizes, the two scintillators (pictured in Figure 2-1) were calculated to have very similar masses, 230 g for the $LaBr_3$:Ce and 234 g for the NaI(Tl), allowing a valid direct comparison. Readout of the $LaBr_3$:Ce detector was accomplished with an ORTEC DART portable multi-channel analyzer (ORTEC, Oak Ridge, TN) with a 0.5 µs shaping time using the same number of channels (1024) as the GR-135. Though the GR-135 has isotope identification software, for our measurements its output files were converted to ORTEC's "*.chn" file format to facilitate comparison. All analysis was done using ORTEC ScintiVision™-32 software.

GR-135

$LaBr_3$:Ce

Figure 2-1. The Two Detectors Compared in this Study

Figure 2-2 shows ^{232}Th spectra from the $LaBr_3$:Ce (upper) and NaI(Tl) (lower) vertically offset from each other so that both are visible. Of particular note is $LaBr_3$:Ce's separation of the 911- and 969-keV peaks at the right side of the figure, compared with that of the NaI(Tl). Also, several minor gamma-ray signatures, such as the 209- and 300-keV gamma rays, are distinguishable in the $LaBr_3$:Ce spectrum that are not in the NaI(Tl) spectrum. Figure 2-3 shows the resolutions measured with the two detectors with the gains set to encompass all energies of interest (up to ~ 3000 keV). For the two detectors compared in this study, the $LaBr_3$:Ce scintillator had better resolution than the NaI(Tl) down to the lowest energy measured at ^{241}Am's 60-keV gamma ray, in contrast with previous studies mentioned earlier. This is because the NaI(Tl) detector, though it had good resolution at energies of 100's of keV, had poorer

(a) Personal communication with M. Mayhugh, Saint-Gobain Crystals and Detectors.

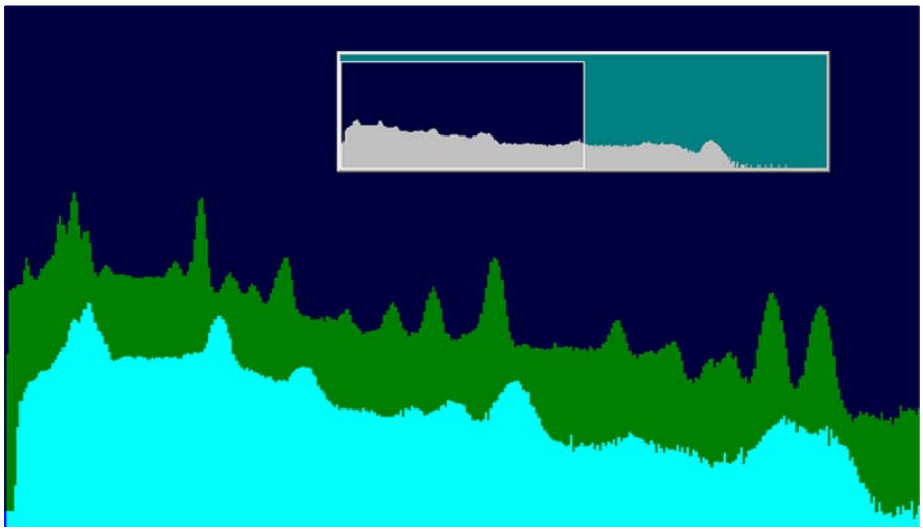

Figure 2-2. ^{232}Th Spectra from $LaBr_3$:Ce (upper) and NaI(Tl) (lower)

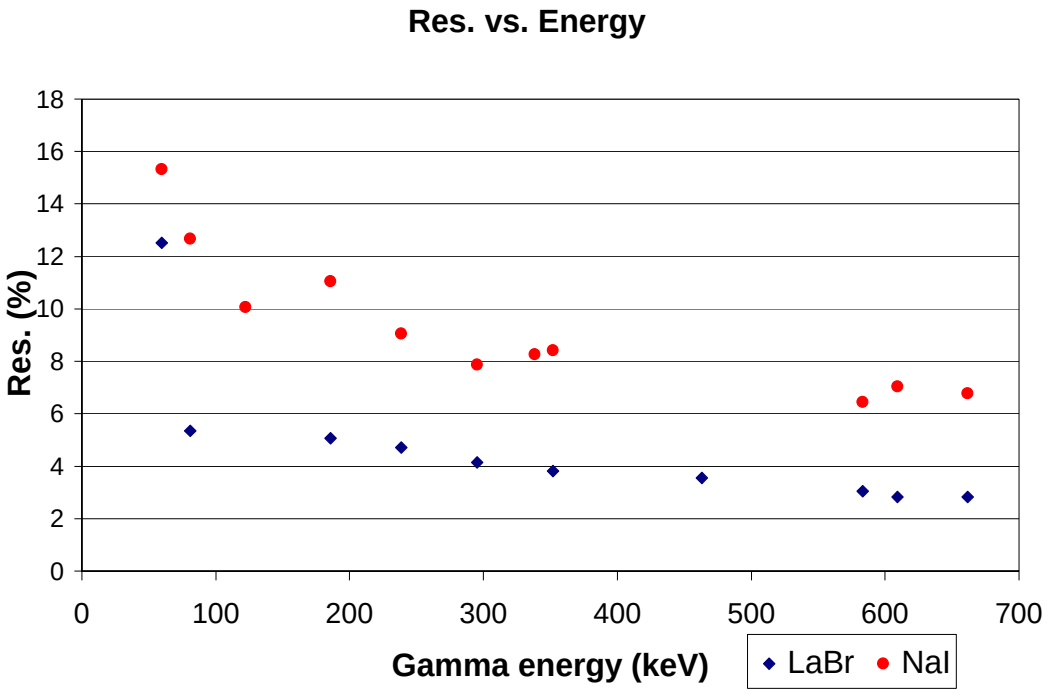

Figure 2-3. Resolution of the two Detectors in the Energy Range 60–662 keV

resolution at lower energies than typical of NaI(Tl). While the gain and channel number settings on the GR-135 are not optimized for low-energy resolution measurements using only a small number of channels, measurements performed with similar NaI(Tl) detectors revealed that only limited improvement is possible by better choice of gain and channel number. Thus the poor resolution is due to the detector itself.

Figure 2-4 shows a 60,000 second unshielded background spectrum taken with the $LaBr_3$:Ce detector, revealing the effects of the internal contaminants mentioned earlier. There is a substantial x-ray peak at 30-40 keV. The peak in the center of the spectrum, at approximately 1468 keV, is the 1436-kev gamma ray, often with a coincident x-ray. One can even note structure depending on whether a coincident x-ray was detected or not. This gamma ray is of particular concern for RIID applications because it is unresolvable from the naturally ubiquitous 1461-keV gamma ray from ^{40}K. The spectrum's broad feature at 750 to 1000 keV is the 789-keV gamma ray in coincidence with a beta particle. All of these are due to the internal ^{138}La. The net count rates for the x-ray peak, the 789-kev gamma-plus-beta hump, and the 1436-kev gamma-plus-x-ray peak are 18.1, 2.7, and 3.1 counts per second, respectively. Above the 1436-keV gamma-plus-x-ray peak in energy are many peaks (1550–3000 keV) associated with the alpha decays from ^{227}Ac. The gross count rate, in this case is 1.5 counts per second. The small bumps between 250-650 keV are true background gamma rays, such as the 609-kev and 352-keV gamma rays from the ^{238}U decay chain. In a NaI(Tl) detector background spectrum, one typically only sees peaks from naturally occurring ^{40}K and the ^{238}U and ^{232}Th decay chains because NaI(Tl) detectors have very little internal contamination.

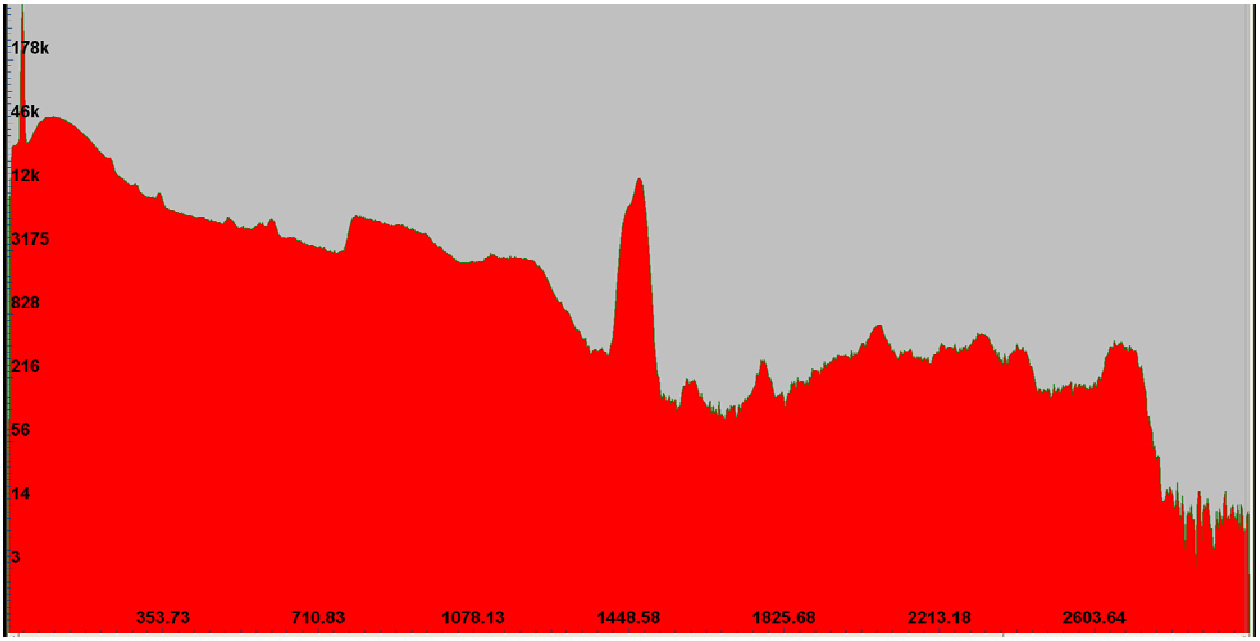

Figure 2-4. 60,000 s Background Spectrum from $LaBr_3$:Ce Detector

The GR-135 gain-stabilizes its spectra, while the $LaBr_3$:Ce's spectra were not stabilized. At the start of a measurement session, a nominal effort was made to ensure approximate alignment of the spectra of the two detectors. Typically, however, the $LaBr_3$:Ce's spectra soon shifted due to the large temperature changes it experienced because most of the measurements were taken outside or in a building with no climate control. $LaBr_3$:Ce's response is fairly stable with temperature (Dathy 2005), so the bulk of the gain-shift observed was presumably due to the photomultiplier tube, underscoring the reality that all RIIDs must be gain-stabilized, and any based on $LaBr_3$:Ce will be no exception. This could be undertaken using a light emitting diode (Pausch et al. 2005) or the signals from the internal contamination (McIntyre et al. 2006). One caveat to the latter approach is that the 1436-keV gamma ray from ^{138}La is often in coincidence with an x-ray, making that peak rather broad.

Using the two detectors, measurements were taken to facilitate comparison under identical circumstances. Measurements included standard radioactive sources, NORM typically found in cargo, and special nuclear materials. Measurements were taken for a variety of times and distances typifying RIID usage. Some measurements involved cargo shielding scenarios and some involved direct contact.

3.0 ANALYSIS

Using the ScintiVision™ software, an attempt was made to compare and quantify, in terms of speed and signal significance, the two detectors' abilities to find spectral peaks. Each spectrum was analyzed using the most accurate calibration curve that could be determined, rather than a set calibration across the measurements. The software was asked to locate all peaks. For those found the signal and background counts were then determined using regions of interest defined "by eye" rather than by the peak finding algorithms. Individual elements of the findings must be viewed as somewhat subjective and dependent on the software used (and software-usage skills of the authors), but this should not affect the overall conclusions. The experience of the authors is that peak finding software for scintillators, in general, does not perform to the level of the "trained eye"; but though this is an active area of study, it was not part of this study.

ScintiVision™ (and many other spectroscopic software codes) calculates a filtered spectrum to find peaks. These peaks are compared to the background uncertainty under the peak (to first order, given by the square root of the background) and must exceed the background uncertainty by a set amount before being further analyzed using peak fitting algorithms to better determine the precise signal count numbers (ORTEC 2002). Thus, an important quantity in the comparative analysis that follows is the "significance" of a peak as related to finding it, given by:

$$\mathrm{Sig}_{\mathrm{find}} = \text{net counts} / \sqrt{\text{background}}$$

Often detectors are used not only to find isotopes (by finding their peaks in spectra), but to measure activities. The "significance" of a peak as related to precisely quantifying it is given by:

$$\mathrm{Sig}_{\mathrm{quan}} = \text{net counts} / \text{net error}$$

The net error is approximated by:

$$\text{net error} \approx \sqrt{\text{background} + \text{gross area}}$$

where gross area is the total counts in a peak (net plus background). In our analysis we use the net error as calculated by ScintiVision™, which differs slightly due to background fitting.

Because net (signal) and background counts are measured simultaneously, both of the above peak significances are proportional to the square root of the measurement time—one must increase the time of measurement by a factor of four to double the significance of the measurement. Likewise, if one detector can measure a significance of twice as much as a second detector in the same amount of time for the same physical setup, it can measure the same significance as the second detector in one fourth the time.

It should be noted that the above equations are derived assuming Gaussian statistics (number of background counts greater than approximately 20), a condition which doesn't always hold in the following analysis, but still provides a useful comparison. Also, the quantitative value of Sig_{find} is more meaningful in cases where the number of net counts is small compared to the number of background counts, and finding peaks is more difficult; though the following analysis includes some measurements where the number of net counts is indeed substantial compared to the background counts.

3.1 Sealed Sources

Table 3-1 compares the two detectors for identical measurements of sealed button sources, at 10 seconds and 100 cm (except, as noted, the ^{241}Am and ^{109}Cd were taken at 10 cm). Ten

Table 3-1. Comparison of $LaBr_3$:Ce and NaI(Tl) Detectors for 10-Second Sealed Source Measurements

			LaBr (100cm, 10sec.)				NaI (100cm, 10sec.)					Comparison
Isotope	Energy	Activity	(Cd-109 and Am-241 data taken at 10cm.)				(Cd-109 and Am-241 data taken at 10cm.)					
	(keV)	(μCi)	Gross Area	Net Area	Backgrd.	Sig_find	Gross Area	Net Area	Backgrd.	Sig_find		(S1/S2)^2
Am-241	59.54	9.8	10600	9644	956	311.9	7059	6261	798	221.6		1.98
Ba-133	81.01	28.8	554	213	341	11.5	504	124	380	6.4		3.29
Cd-109	88.04	6.7	797	473	324	26.3	618	374	244	23.9		1.20
Co-57	122.07	37.1	1228	749	479	34.2	1186	526	660	20.5		2.79
Ba-133	276.29	28.8	86	30	56	4.0						
Ba-133	302.71	28.8	126	43	83	4.7						
Ba-133	355.86	28.8	421	330	91	34.6	418	318	100	31.8		1.18
Ba-133	383.70	28.8	49	16	33	2.8						
Cs-137	661.62	9.1	93	78	15	20.1	110	96	14	25.7		0.62
Co-60	1172.23	7.1	51	36	15	9.3	35	19	16	4.8		3.83
Co-60	1332.51	7.1	30	19	11	5.7	28	16	12	4.6		1.54
											Average	2.05
											Std Dev	1.14

seconds was the shortest time period that the GR-135 could be set to acquire. Those blocks in red represent peaks that the software was unable to find, which only happened with the NaI(Tl) detector. The last column calculates the square of the ratio of the $LaBr_3$:Ce Sig_{find} value over the NaI(Tl) Sig_{find} value. This value gives the time multiplier necessary for the NaI(Tl) detector to measure a significance equal to that of the $LaBr_3$:Ce detector. On average the NaI(Tl) would have needed a measurement 2.05 times longer to achieve the same significance as the $LaBr_3$:Ce. Conversely, the $LaBr_3$:Ce could have measured to the same amount of significance in approximately half the time as the NaI(Tl). Table 3-2 agrees with this conclusion, comparing a 5 second measurement of $LaBr_3$:Ce with the 10-second NaI(Tl) measurement. The $LaBr_3$:Ce is still able to find all of the peaks and a comparison of the Sig_{find} values implies that the two detectors are finding peaks with equal significance, though the standard deviation on the comparison ratio is quite large.

Table 3-2. Comparison of 5 Second $LaBr_3$:Ce Measurements Versus 10 Second NaI(Tl) Measurements for Sealed Sources

			LaBr (100cm, 5sec.)				NaI (100cm, 10sec.)					Comparison
Isotope	Energy	Activity	(Cd-109 and Am-241 data taken at 10cm.)				(Cd-109 and Am-241 data taken at 10cm.)					
	(keV)	(μCi)	Gross Area	Net Area	Backgrd.	Sig_find	Gross Area	Net Area	Backgrd.	Sig_find		(S1/S2)^2
Am-241	59.54	9.8	5380	4927	453	231.5	7059	6261	798	221.6		1.09
Ba-133	81.01	28.8	271	119	152	9.7	504	124	380	6.4		2.30
Cd-109	88.04	6.7	412	265	147	21.9	618	374	244	23.9		0.83
Co-57	122.07	37.1	643	391	252	24.6	1186	526	660	20.5		1.45
Ba-133	276.29	28.8	44	15	29	2.8						
Ba-133	302.71	28.8	69	44	25	8.8						
Ba-133	355.86	28.8	200	126	74	14.6	418	318	100	31.8		0.21
Ba-133	383.70	28.8	28	16	12	4.6						
Cs-137	661.62	9.1	39	29	10	9.2	110	96	14	25.7		0.13
Co-60	1172.23	7.1	18	14	4	7.0	35	19	16	4.8		2.17
Co-60	1332.51	7.1	19	6	13	1.7	28	16	12	4.6		0.13
											Average	1.04
											Std Dev	0.88

Table 3.3 shows a comparison of the two detectors for 60 second measurements, where for this longer measurement we are comparing Sig_{quan} rather than Sig_{find}. Again, the NaI(Tl) detector was unable to find a few of the ^{133}Ba peaks. The $LaBr_3$:Ce detector was able to make measurements of equal significance over twice as fast as the NaI(Tl) detector.

Table 3-3. Comparison of $LaBr_3$:Ce and NaI(Tl) Detectors for 60-Second Sealed Source Measurements

			LaBr (100cm, 60sec.)				NaI (100cm, 60sec.)				Comparison
Isotope	Energy	Activity	(Cd-109 and Am-241 data taken at 10cm.)				(Cd-109 and Am-241 data taken at 10cm.)				
	(keV)	(μCi)	Gross Area	Net Area	Error	Sig_quan	Gross Area	Net Area	Error	Sig_quan	(S1/S2)^2
Am-241	59.54	9.8	63295	57461	251	228.9	41864	37696	209	180.4	1.61
Ba-133	81.01	28.8	3166	1165	42	27.7	2724	561	35	16.0	2.99
Cd-109	88.04	6.7	5173	3221	64	50.3	3597	1717	54	31.8	2.51
Co-57	122.07	37.1	6836	3942	73	54.0	6878	3270	79	41.4	1.70
Ba-133	276.29	28.8	560	171	22	7.8					
Ba-133	302.71	28.8	858	309	24	12.9	1397	323	51	6.3	4.13
Ba-133	355.86	28.8	2247	1759	48	36.6	2554	1582	67	23.6	2.41
Ba-133	383.70	28.8	348	76	16	4.8					
Cs-137	661.62	9.1	558	428	28	15.3	541	398	32	12.4	1.51
Co-60	1172.23	7.1	336	226	25	9.0	297	212	26	8.2	1.23
Co-60	1332.51	7.1	225	183	18	10.2	205	130	21	6.2	2.70
										Average	2.31
										Std Dev	0.91

Table 3-4 compares the two detectors for longer measurements with and without shielding between the sources and detector. The shielding in this case is one-half inch steel. The comparison calculation includes a time factor because the measurement times were not identical. As before, the calculated values relate how much faster the $LaBr_3$:Ce detector can measure a peak to a particular significance than the NaI(Tl). As expected, the shielding eliminates detection of the lower-energy gamma rays and reduces detection of higher energy gamma rays. The shielding does not greatly change the comparison of the detectors with respect to each other.

Table 3-4. Comparison of $LaBr_3$:Ce and NaI(Tl) Detectors for Shielded Sealed Source Measurements

			LaBr(100cm, 180sec., bare)				NaI(100cm, 200sec., bare)					Comparison
Isotope	Energy (keV)	Activity (µCi)	Gross Area	Net Area	Error	Sig_quan	Gross Area	Net Area	Error	Sig_quan		(t2/t1)*(S1/S2)^2
Am-241	59.54	9.8	4280	1665	58	28.7	3384	1632	62	26.3		1.32
Ba-133	81.01	28.8	12653	5023	112	44.8	11722	4587	113	40.6		1.36
Co-57	122.07	37.1	20390	11730	126	93.1	24814	13824	168	82.3		1.42
Ba-133	276.29	28.8	2010	548	39	14.1						
Ba-133	302.71	28.8	3195	1757	56	31.4	6486	2151	134	16.1		4.24
Ba-133	355.86	28.8	6890	5439	85	64.0	8830	5459	154	35.4		3.62
Ba-133	383.70	28.8	1349	449	34	13.2						
Cs-137	661.62	9.1	1919	1411	54	26.1	1941	1475	65	22.7		1.47
Co-60	1173.23	7.1	990	637	44	14.5	1120	600	67	9.0		2.90
Co-60	1332.51	7.1	637	564	29	19.4	759	567	42	13.5		2.31
											Average	2.33
											Std Dev	1.15

			LaBr(100cm, 180sec., 1/2" steel)				NaI(100cm, 200sec., 1/2" steel)					Comparison
Isotope	Energy (keV)	Activity (µCi)	Gross Area	Net Area	Error	Sig_quan	Gross Area	Net Area	Error	Sig_quan		(t2/t1)*(S1/S2)^2
Am-241	59.54	9.8										
Ba-133	81.01	28.8										
Co-57	122.07	37.1	4990	1499	66	22.7	5995	1622	90	18.0		1.76
Ba-133	276.29	28.8	1703	262	38	6.9						
Ba-133	302.71	28.8	2169	620	49	12.7	3699	631	99	6.4		4.38
Ba-133	355.86	28.8	3608	2245	63	35.6	4676	2393	110	21.8		2.98
Ba-133	383.70	28.8	832	144	26	5.5						
Cs-137	661.62	9.1	1119	622	41	15.2	1134	601	60	10.0		2.55
Co-60	1173.23	7.1	732	495	39	12.7	668	372	43	8.7		2.39
Co-60	1332.51	7.1	451	397	25	15.9	488	317	36	8.8		3.61
											Average	2.95
											Std Dev	0.93

3.2 Special Nuclear Materials

For comparison of the two detector materials for special nuclear materials, a 98 g weapons-grade plutonium (WGPu) source and a123 g highly-enriched uranium (HEU) (93.1 percent ^{235}U) source were used. Table 3-5 displays results for the WGPu. The values range widely, but always favor the $LaBr_3$:Ce detector. The NaI(Tl) detector, in particular, had trouble with the ^{239}Pu gamma-ray complex in the 300- and 400-keV regions due to its inferior resolution. Table 3-5 also shows results for the detectors performing measurements of the WGPu behind one inch of steel. Both detectors were unable to detect peaks below 300-keV that they had detected when no shielding was in place. Again, $LaBr_3$:Ce performed significantly better for those peaks that both detectors found.

Table 3-5. Comparison of $LaBr_3$:Ce and NaI(Tl) for WGPu Measurements

	LaBr (100cm, 300sec.)					NaI (100cm, 200sec.)					Comparison
Energy (keV)	FWHM	Gross Area	Net Area	Error	Sig_quan	FWHM	Gross Area	Net Area	Error	Sig_quan	(t2/t1)*(S1/S2)^2
51.64	6.54	44970	11402	183	62.3	7.06	29643	4407	159	27.7	3.37
98.78	9.83	101838	20693	297	69.7	12.97	71392	12043	285	42.3	1.81
203.54	10.95	32920	4848	181	26.8	13.70	26973	1686	176	9.6	5.21
332.81	21.22	27588	9119	199	45.8	11.62	21595	1617	195	8.3	20.36
375.02	15.35	35627	17536	218	80.4	4.46	23008	1420	183	7.8	71.64
413.69	13.29	20755	9950	161	61.8	1.99	14168	667	128	5.2	93.77
451.44	12.67	3707	1229	78	15.8						
	LaBr (100cm, 180sec., 1" steel)					NaI (100cm, 200sec., 1" steel)					Comparison
Energy (keV)	FWHM	Gross Area	Net Area	Error	Sig_quan	FWHM	Gross Area	Net Area	Error	Sig_quan	(t2/t1)*(S1/S2)^2
51.64											
98.78											
203.54											
332.81	8.00	4428	688	79	8.7	4.44	5857	372	97	3.8	5.73
375.02	15.71	4885	1572	80	19.7	22.81	5919	527	97	5.4	14.53
413.69	12.37	2977	1034	62	16.7	8.74	3151	167	56	3.0	34.75
451.44	7.55	858	130	36	3.6						

Table 3-6 shows the HEU results for the 186-keV gamma ray. The blue rows represent when no measurement was made for that time-setting. As has been seen before, the $LaBr_3$:Ce detector could measure peaks to the same significance as the NaI(Tl) detector approximately twice as fast.

Table 3-6. Comparison of $LaBr_3$:Ce and NaI(Tl) for HEU Measurements

		LaBr (100 cm)					NaI (100 cm)					Comparison
Time (s)	Shielding	Gross Area	Net Area	Error	Res. (%)	Sig_quan	Gross Area	Net Area	Error	Res. (%)	Sig_quan	(t2/t1)*(S1/S2)^2
60	bare	2642	1147	58	4.5	19.8	3425	1497	83	10.2	18.0	1.20
180	bare	7066	3798	84	5.0	45.2						
200	bare						10808	4358	139	9.6	31.4	2.31
60	1" steel	753	88	29	4.0	3.0	1220	105	55	11.1	1.9	2.53
180	1" steel	2325	284	51	5.1	5.6						
200	1" steel						3435	348	86	10.5	4.0	2.10

3.3 ^{40}K NORM

As mentioned earlier, the 1436-keV gamma ray from ^{138}La found in lanthanum halide detectors is of particular concern for RIID applications. This gamma ray, which is often detected in coincidence with a Ba x-ray, is indistinguishable from the 1461-keV gamma ray from ^{40}K. Not only is ^{40}K prevalent in the natural background, but as such it is also found in many items of commerce, including fertilizer, kitty litter, tile, ice melt, and concrete. It is the most common radioisotope identified by RIIDs at U.S. Port of Entry by Customs officers (Bates and Woodring 2004), although this is partly due to RIIDs frequently "identifying" the background radiation (Woodring et al. 2004, Seitz et al. 2005). For background measurement situations, a MCNPX (Pelowitz 2005) simulation attributed 80 percent of the counts to ^{138}La and 20 percent to the background, 80 percent of which was due to ^{40}K.

Table 3-7 compares the LaBr3:Ce and NaI(Tl) detectors for 300-second measurements taken 100 cm from 1 m^3 containers of various ^{40}K-containing NORMs. Results from the comparable background measurement are subtracted from the measurements to give net counts that are due to the NORM and not the ^{40}K (and ^{138}La, in the case of $LaBr_3$:Ce) background. The tile and kitty litter were too weak to be discernable from background. The significance in the table refers to the net counts over the square root of the original (gross) area (net plus background). Because of the ^{138}La internal contamination, the NaI(Tl) is superior at measuring the ^{40}K from NORM and can make a measurement to the same level of significance in less time. Table 3-8 makes the same comparison, but with the detector in contact with the NORM containers, and for a longer measurement time. Again, kitty litter could not be distinguished from background, though tile could in this case. With the higher ^{40}K activity (due to proximity), $LaBr_3$:Ce's contamination becomes less of a factor, but NaI(Tl) still performs better.

Table 3-7. Comparison of $LaBr_3$:Ce and NaI(Tl) for Standoff ^{40}K Measurements

	LaBr (100 cm, 300 sec.)			NaI (100 cm, 300 sec.)			
Source	**Orig. Area**	**Net Area**	**Sig**	**Orig Area**	**Net Area**	**Sig**	**(S1/S2)^2**
ice melt	1706	663	16.1	710	545	20.5	0.62
fertilizer	1160	117	3.4	305	140	8.0	0.18
tile	1045	2	0.1	144	-21	-1.8	
kitty litter	1007	-36	-1.1	129	-36	-3.2	
background	1043			165			

Table 3-8. Comparison of $LaBr_3$:Ce and NaI(Tl) for Contact ^{40}K Measurements

	LaBr (contact, 1200 sec.)			NaI (contact, 1200 sec.)			Comparison
Source	**Orig. Area**	**Net Area**	**Sig**	**Orig Area**	**Net Area**	**Sig**	**(S1/S2)^2**
ice melt	19035	14953	108.4	14183	13577	114.0	0.90
fertilizer	6368	2286	28.6	2524	1918	38.2	0.56
tile	4559	477	7.1	1035	429	13.3	0.28
kitty litter	3491	-591	-10.0	454	-152	-7.1	
background	4082			606			

It is important to understand the relevance of how "significance" was defined for these tables. The ^{138}La contamination contributes to this (~1461 keV) and other regions of the detector's spectra at a steady rate which can be determined to a very precise level (i.e., very little statistical error) by measuring it over a long time period. If the background is indeed very precisely known, the net error on a peak no longer depends on both the gross area and the background (as defined in Section 3.0), but only the gross area. (This disregards other contributions to the "background" of a spectrum, such as the natural radioactive background of the location where the detector was used.) The contamination's effect is not completely eliminated, however, no matter how well the contamination is quantified – it still contributes to the gross area of the peak from which the ^{40}K net area must be extracted. Certainly as the source signal (net area) becomes larger relative to the contamination background, its performance improves, but even for our contact 1 m^3 NORM measurements, the source signals were not robust enough for the $LaBr_3$:Ce to perform better than the NaI(Tl). For ice melt on contact, the LaBr3:Ce performed almost as well as the NaI(Tl), and would presumably perform better for larger volumes.

3.4 ^{226}Ra and ^{232}Th

Like ^{40}K, the ^{238}U and ^{232}Th decay-chains are naturally-occurring and typically seen in background spectra and "earth-based" NORM, such as granite and pottery. Unlike ^{40}K, these isotopes have long decay schemes and the spectra involve many daughter isotopes, but are typically collectively referred to by RIIDs as ^{226}Ra and ^{232}Th. The gamma spectrum for ^{226}Ra is essentially identical to that of ^{238}U for the resolutions that scintillators can achieve, and ^{226}Ra can be made into smaller calibration sources due to its shorter half-life. Thus most RIIDs refer to this series as "^{226}Ra." After ^{40}K and a few medical isotopes, ^{226}Ra and ^{232}Th are the most commonly identified isotopes by RIIDs at U.S. Port of Entry by Customs officers (Bates and Woodring 2004).

For our study of these two isotopes, we had hoped to use NORM like it was used for ^{40}K. We did not, however, have m^2 samples in this case, only small pieces of granite and uranium glass, which had insufficient activity for this study. Calibrated sources were used instead, in particular a 1.6 μCi ^{226}Ra button source and an 8.1 μCi "tuna can" ^{232}Th source.

Table 3-9 compares the LaBr3:Ce and NaI(Tl) detectors for the ^{226}Ra source for various measurement distances and times. Those blocks in red represent peaks that the software was unable to find. The background values are not shown, but they were used to calculate Sig_{find} for energies where both detectors were able to measure the peaks. The comparison values are consistent with those found previously.

Table 3-9. Comparison of $LaBr_3$:Ce and NaI(Tl) for ^{226}Ra Measurements

Net Area

LaBr		Energy (keV)											
Dist. (cm)	Time (s)	185.99	241.92	295.22	351.99	609.32	768.35	934.04	1120.27	1238.10	1764.51	2204.50	2447.68
10	30	590	622	1119	1900	1515	83	n/a	242	41	n/a	34	7
10	300	4910	5790	13879	23526	15566	1215	501	2269	730	1559	450	96
100	300	n/a	n/a	n/a	n/a	336	n/a	n/a	142	35	n/a	n/a	n/a
NaI													
10	30	n/a	444	1068	1795	1103	n/a	n/a	143	n/a	n/a	n/a	n/a
10	300	3684	4385	9679	16769	11747	1871	n/a	1853	431	835	n/a	n/a
100	300	n/a	n/a	n/a	n/a	285	n/a	n/a	n/a	n/a	n/a	5	n/a

Sig_find

LaBr		Energy (keV)											
Dist. (cm)	Time (s)	185.99	241.92	295.22	351.99	609.32	768.35	934.04	1120.27	1238.10	1764.51	2204.50	2447.68
10	30	13.96	16.92	32.91	55.96	70.71	3.49		14.21	2.57		6.01	4.95
10	300	38.15	59.71	146.38	267.70	226.28	18.84	7.93	38.83	13.50	42.51	28.02	12.50
100	300					12.05			6.69	2.20			
NaI													
10	30		9.69	23.45	39.05	42.11			6.62				
10	300	21.88	28.62	65.16	122.39	139.88	15.75		30.84	6.10	19.97		
100	300					8.34						2.50	

Comparison

(S1/S2)^2		Energy (keV)											
Dist. (cm)	Time (s)	185.99	241.92	295.22	351.99	609.32	768.35	934.04	1120.27	1238.10	1764.51	2204.50	2447.68
10	30		3.05	1.97	2.05	2.82			4.60				
10	300	3.04	4.35	5.05	4.78	2.62	1.43		1.59	4.90	4.53		
100	300					2.09							
		Average	3.26										
		Std Dev	1.31										

Table 3-10 compares the two detectors for the ^{232}Th source. The NaI(Tl) detector was unable to resolve the 911- and 969-keV peaks, though the collective peak is clearly seen. The counts of the collective peak are listed together (under 911 keV) for the NaI(Tl) detector, but these results are not compared with the $LaBr_3$:Ce detector. For the 2614-keV peak, there were often no background counts (as determined by the software). With no background, the Sig_{find} variable is meaningless and shown in yellow in the table. As before, peaks that were not found are shown in red and the $LaBr_3$:Ce detector consistently performed better. Of course, a RIID would not need all of the peaks listed in the last two tables to identify ^{226}Ra or ^{232}Th, rather the use of these multi-peaked sources probes the ability of the detectors in multi-peak (i.e., multi-source) situations.

Table 3-10. Comparison of $LaBr_3$:Ce and NaI(Tl) for ^{232}Th Measurements

Net Area

LaBr		Energy (keV)									
Dist. (cm)	Time (s)	238.63	338.42	463.10	510.72	583.14	727.17	911.07	968.97	1588.23	2614.47
10	10	2350	857	240	373	983	108	500	442	147	265
10	60	15302	4574	1016	2176	5977	1028	3261	2634	915	1571
100	60	414	182	64	54	120	n/a	108	83	19	46
100	180	1178	328	107	127	379	48	259	272	n/a	124
NaI											
10	10	1900	497	127	136	786	101	878	inc. 911	148	240
10	60	9404	2616	335	784	3259	338	3784	inc. 911	818	1109
100	60	252	85	n/a	n/a	174	n/a	136	inc. 911	n/a	37
100	200	939	353	n/a	143	427	n/a	647	inc. 911	n/a	156

Sig_find

LaBr		Energy (keV)									
Dist. (cm)	Time (s)	238.63	338.42	463.10	510.72	583.14	727.17	911.07	968.97	1588.23	2614.47
10	10	58	27	10	16	36	5	28	32	15	no back
10	60	145	58	17	37	95	22	86	87	35	214
100	60	17	11	5	4	9		9	8	4	11
100	180	28	10	5	6	17	3	14	14		25
NaI											
10	10	33	12	5	5	24	4	37		10	no back
10	60	76	28	5	13	46	7	68		23	94
100	60	8	4			12		11			no back
100	200	16	8		5	16		31			no back

Comparison

(t2/t1)*(S1/S2)^2		Energy (keV)									
Dist. (cm)	Time (s)	238.63	338.42	463.10	510.72	583.14	727.17	911.07	968.97	1588.23	2614.47
10	10	3.13	5.15	4.69	9.90	2.31	1.41			2.43	
10	60	3.64	4.33	12.54	8.64	4.28	10.22			2.36	5.13
100	60	4.05	6.87			0.50					
100	180-200	3.34	1.60		1.35	1.31					
		Average	4.51								
		Std Dev	3.25								

4.0 CONCLUSIONS

We have performed a comparison study of a NaI(Tl)-based RIID and a comparably sized LaBr3:Ce detector to assess the effect this new material may have on hand-held detector performance. Measurements were taken for short time frames, as typifies RIID usage. Measurements included examples of NORM typically found in cargo and special nuclear materials. Some measurements were non-contact, involving short distances or cargo shielding scenarios. To facilitate direct comparison, spectra from the different detectors were analyzed with the same isotope identification software.

As one would expect, given LaBr3:Ce's higher resolution (3 percent versus 6.5 percent for NaI(Tl) at 662 keV), and higher efficiency (due to higher Z-content), LaBr3:Ce was able to detect more peaks and detect them faster than the NaI(Tl)—approximately 2 to 3 times faster for the same level of significance. This was true for a variety of calibration sources and special nuclear material, shielded or unshielded. The noticeable exception was for 40K, due to 138La internal contamination in LaBr3:Ce. Even for 40K-containing NORM with fairly robust signatures, NaI(Tl) was superior at detection of this important isotope.

Another potential drawback of LaBr3:Ce detectors, their lower resolution at low-energies, was found not to be an issue in this comparison, due to the lower-than-expected resolution of the NaI(Tl) detector in this region. The current cost of LaBr3:Ce detectors is currently much more than NaI(Tl) detectors, though this cost-difference is expected to diminish (but not completely) with time.

As is true of all detectors, the material will need to be gain-stabilized for RIID applications. This could possibly be done using the internal contaminants themselves. It is the experience of the authors that peak finding software in RIIDs needs to be improved, regardless of the detector material. Also, RIIDs must ensure that they have adequate background statistics before identifying the 40K "signal". This will be especially true for LaBr3:Ce-based systems.

5.0 REFERENCES

American National Standard Institute. 2003. *Performance Criteria for Hand-Held Instruments for Detection and Identification of Radionuclides*. ANSI N42.34-2003, ANSI, Washington, D.C.

Balcerzyk M, M Moszynski, and M Kapusta. 2005. "Comparison of $LaCl_3$:Ce and NaI(Tl) scintillators in gamma-ray spectroscopy." *Nuc. Inst. and Meth. A*, vol. 537, pp. 50-6.

Bates D and M Woodring. 2004. *Initial Metadata Analysis for Northern Border Ports of Entry*. PNNL-14757. Pacific Northwest National Laboratory, Richland, Washington.

Dathy C. 2005. Saint-Gobain letter to customer. Available at www.detectors.saint-gobain.com/Media/Documents/S00000000000000001004/BrilLanCeLetterOctober2005.pdf.

Dorenbos P, JTM De Haas, and CWE van Eijk. 2004. "Gamma-ray spectroscopy with a ∅19 × 19 mm3 LaBr3:0.5%Ce3+ scintillator." *IEEE Trans. Nuclear Science*, 51(3):1289-96.

Firestone RB and LP Ekstrom. January 2004. "WWW Table of Radioactive Isotope," Version 2.1. Available at http://ie.lbl.gov/toi/index.asp.

Hartwell JK and RJ Gehrke. 2005. "Observations on the background spectra of four $LaCl_3$(Ce) scintillation detectors." *App. Rad. and Iso.,* vol. 63, pp. 223-8.

Iltis A, G Gautier, JF Nee, and CJ Kaufman. October 2004. "Recent progress in $LaCl_3$:10%Ce^{3+} high energy background and x-rays energy resolution." *IEEE NSS Conference*, Rome.

Kernan WJ. October 2004. "Self-Activity of Lanthanum Halides." *IEEE NSS Conference*, Rome.

Kouzes RT. 2004. "Radiation detection and interdiction for public protection from terrorism." *Public Protection from Nuclear, Chemical, and Biological Terrorism*, A Brodsky and RH Johnson Jr (Eds.). Medical Physics Publishing, Madison, Wisconsin.

McDonald JC, BM Coursey, and M Carter. November 2004. "Detecting illicit radioactive sources." *Physics Today*, 57(11):36-41.

McIntyre JI, BT Schrom, TW Bowyer, MW Cooper, TR Day, JC Hayes, TR Heimbigner, CW Hubbard, BD Milbrath, MD Ripplinger, and R Suarez, April 2006. "Using beta-gamma coincidence signatures of entrained radioactive contaminants to calibrate radiation detectors." *MARC VII Conference*, Kona, Hawaii.

Milbrath BD, JI McIntyre, RC Runkle, and LE Smith. 2005a. *Contamination in $LaCl_3$:Ce Scintillators*. PNNL-15453. Pacific Northwest National Laboratory, Richland, Washington.

Milbrath BD, RC Runkle, TW Hossbach, WR Kaye, EA Lepel, BS McDonald, and LE Smith. 2005b. "Characterization of alpha contamination in lanthanum trichloride scintillators using coincidence measurements." *Nuc. Inst. and Meth. A*, vol. 547, pp. 504-510.

Milbrath BD, BJ Choate, JE Fast, RL Kouzes, and JE Schweppe. October 2005c. "Comparison of $LaBr_3$:Ce and NaI(Tl) scintillators for radioisotope identification devices." *IEEE NSS Conference*, Fajardo, Puerto Rico.

Pausch G, J Stein, A Kreuels, F Lueck, and N Teofilovl. October 2005. "Multifunctional pulse width analysis in a LED-stabilized digital NaI(Tl) spectrometer." *IEEE NSS Conference*, Fajardo, Puerto Rico.

Pelowitz DB (Ed.). 2005. *MCNPX User's Manual*. LA-CP-05-0369, Los Alamos National Laboratory, Los Alamos, New Mexico.

ORTEC. 2002. ScintiVision™-32 A35-B52 *Software User's Manual*. ORTEC, Oak Ridge, Tennessee.

Seitz SL, JM Blackadar, SK Almecci, and WH Casson. June 2005. "RadAssessor database." LA-UR-05-4325, Los Alamos National Laboratory, Los Alamos, New Mexico.

Shah KS, J Glodo, M Klugerman, WW Moses, SE Derenzo, and MJ Weber. December 2003a. "$LaBr_3$:Ce scintillators for gamma-ray spectroscopy." *IEEE Trans. Nuclear Science,* 50(6):2410-3.

Shah KS, J Glodo, M Klugerman, L Cirignano, WW Moses, SE Derenzo, and MJ Weber. 2003b. "$LaCl_3$:Ce scintillator for gamma-ray detection." *Nuc. Inst. and Meth. A*, vol. 505, pp. 76-81.

Syntfeld A, R Arlt, P Dvornyak, V Gostilo, Z He, A Loupilov, M Moszynski, and M Swoboda. October 2005. "Comparison of a large volume CdZnTe detector with a LaBr-3 detector." *IEEE NSS Conference*, Fajardo, Puerto Rico.

van Eijk CWE. 2001. "New inorganic scintillators – aspects of energy resolution." *Nuc. Inst. and Meth. A*, vol. 471, pp. 244-248.

van Loef EVD, P Dorenbos, CWE van Eijk, K Kramer, and HU Gudel. September 2001a. "High-energy-resolution scintillator: Ce^{3+} activated $LaBr_3$." *Applied Physics Letters*, 79(10):1573-1575.

van Loef EVD, P Dorenbos, and CWE van Eijk. June2001b. "Scintillation properties of $LaCl_3$:Ce^{3+} crystals: fast, efficient, and high-energy resolution scintillators." *IEEE Trans. Nuclear Science*, 48(3):341-345.

Woodring M, J Ely, and RT Kouzes. 2004. "Radioisotope identification device testing for secondary screening applications." PNNL-14782. Pacific Northwest National Laboratory, Richland, Washington.